

Thinking Ahead: Foresight Intelligence in MLLMs and World Models

Zhantao Gong¹ Liaoyuan Fan² Qing Guo¹ Xun Xu³ Xulei Yang³ Shijie Li³

¹Nankai University

²The University of Hong Kong

³Institute for Infocomm Research (I2R), A*STAR, Singapore



Project Page



Evaluation Code



FSU-QA

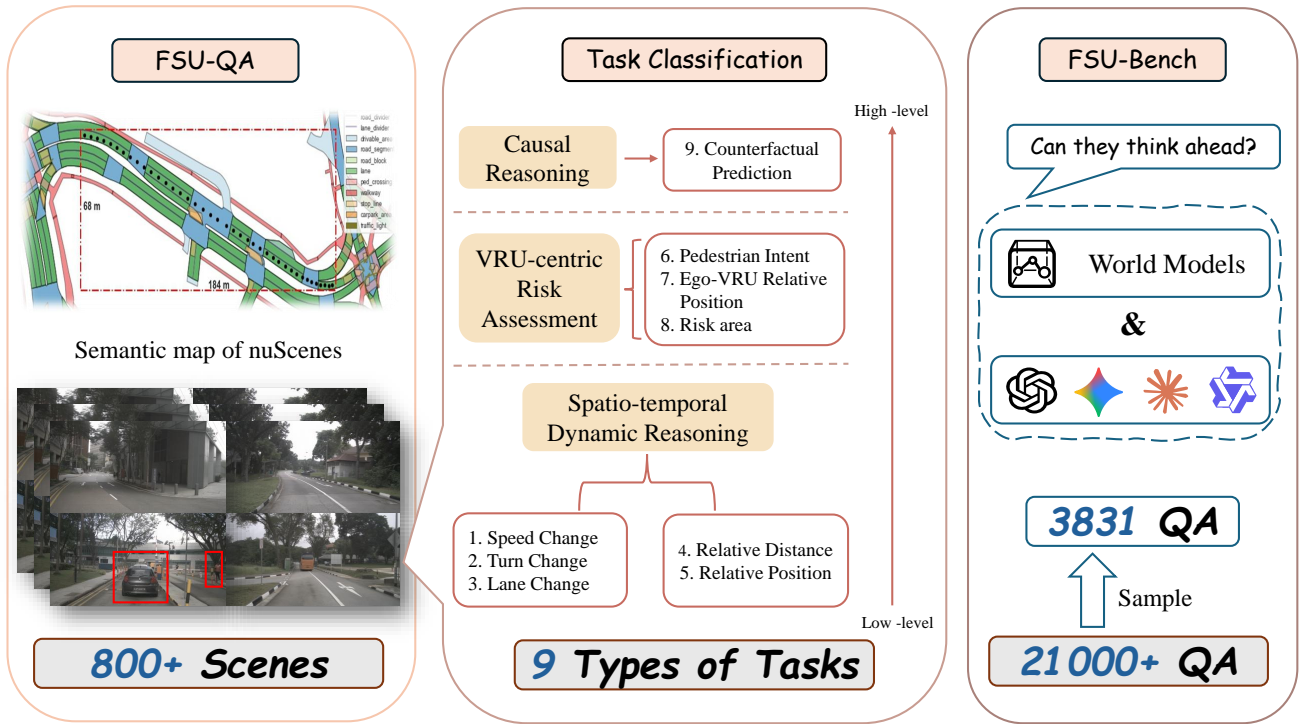


Figure 1. Overview of FSU-QA and FSU-Bench.

Abstract

In this work, we define *Foresight Intelligence* as the capability to anticipate and interpret future events—an ability essential for applications such as autonomous driving, yet largely overlooked by existing research. To bridge this gap, we introduce FSU-QA, a new Visual Question-Answering (VQA) dataset specifically designed to elicit and evaluate Foresight Intelligence. Using FSU-QA, we conduct the first comprehensive study of state-of-the-art Vision-Language Models (VLMs) under foresight-oriented tasks, revealing that current models still struggle to reason about future situations. Beyond serving as a benchmark, FSU-QA also en-

ables the assessment of world models by measuring the semantic coherence of their generated predictions, quantified through performance gains when VLMs are augmented with such outputs. Our experiments further demonstrate that FSU-QA can effectively enhance foresight reasoning: even small VLMs fine-tuned on FSU-QA surpass much larger, advanced models by a substantial margin. Together, these findings position FSU-QA as a principled foundation for developing next-generation models capable of truly anticipating and understanding future events.

1. Introduction

In recent years, Vision-Large Language Models (VLMs) have achieved remarkable progress in visual understanding and cross-modal reasoning [18]. Typically, VLMs integrate a vision encoder with a Large Language Model (LLM) that has been pretrained on large-scale textual corpora rich in common knowledge. This design enables them to excel in both perception and understanding, leading to their widespread application in domains such as robotic perception and scene understanding [31].

Most existing Vision-Language Model (VLM) studies focus on enabling VLMs to understand multimodal data such as 2D/3D scene understanding, spatial reasoning, and video comprehension [7, 14, 23]. However, these works mainly emphasize observed information while neglecting the ability to anticipate and reason about future, unobserved events. This is particularly challenging, as it requires reasoning over complex spatio-temporal information and dealing with multiple plausible futures, which introduces significant uncertainty. We term this concept Foresight Intelligence, which refers to the ability to anticipate and reason about complex future possibilities based on historical observations.

In this work, we present FSU-QA (see Fig. 1), a Visual Question Answering (VQA) dataset, along with its accompanying benchmark, FSU-Bench, designed for training and evaluating Foresight Understanding. Together, they are designed to advance research on Foresight Intelligence. Considering that VLMs are increasingly being integrated into autonomous driving applications, where vehicles must operate in highly dynamic environments and are required to anticipate potential future events to ensure safety, we construct FSU-QA under the autonomous driving scenario. In FSU-QA, we meticulously design the tasks to both train models and comprehensively evaluate their Foresight Intelligence. Specifically, FSU-Bench requires the models to anticipate and interpret potential future scenarios across different temporal intervals based on the current situation, thereby enabling effective evaluation of long-term planning capabilities. The designed tasks are organized according to their cognitive complexity, ranging from low-level perception tasks to mid-level imagination tasks and high-level reasoning tasks, which collectively provide a thorough assessment of foresight intelligence.

FSU-Bench is also designed to evaluate World Models (WMs)’ ability to produce semantically coherent data. Compared to VLMs, which excel at perception and understanding, WMs incorporate physical realism into generative modeling to produce visually realistic future scenarios. Although such data may appear visually realistic, it remains an open question whether they are semantically coherent and can contribute to Foresight Intelligence. In FSU-Bench, several VLMs serve as evaluators to determine whether

the data generated by WMs can improve Foresight Intelligence performance. With such a joint evaluation of VLMs and WMs, a comprehensive assessment of Foresight Intelligence is conducted, aiming to answer two fundamental questions: (1) What is the capability of VLMs in Foresight Intelligence? (2) Can the data generated by WMs contribute to Foresight Intelligence?

A comprehensive evaluation across multiple VLMs and WMs is also conducted, establishing a solid foundation for future research. Our contribution can be summarized as:

- We propose FSU-QA, a dataset designed to train and evaluate the Foresight Intelligence of VLMs through a set of meticulously designed tasks. Our experiments further demonstrate that FSU-QA can effectively enhance VLMs’ foresight reasoning.
- By employing VLMs as evaluators, FSU-Bench further enables the assessment of the semantic coherence of data generated by WMs in foresight understanding tasks.
- Finally, a comprehensive evaluation across multiple VLMs and WMs is conducted on FSU-Bench, establishing a solid foundation for future research.

2. Related Work

The field of multimodal intelligence has witnessed rapid advancements, particularly with the emergence of powerful VLMs and WMs. Our work intersects with and builds upon several key areas of research, including WMs for autonomous driving, multimodal language models, and existing benchmarks for video understanding and autonomous driving.

2.1. Spatio-Temporal Reasoning in VLMs

Modern VLMs have progressed significantly beyond single-frame understanding [27, 35]. Advanced models [20] now demonstrate a strong capacity to capture both temporal information and static spatial relations in videos, achieving robust performance in open dialogue and multimodal reasoning. For instance, Qwen2.5-VL [3] leverage timestamp encoding for long video understanding, while InternVL-3.5 [25] employs a visual resolution router to efficiently process fine-grained video details.

2.2. Benchmarks

To evaluate VLMs’ capabilities, a series of benchmarks have been proposed, but these largely focus on understanding the present state.

- Static Spatial Reasoning: Early benchmarks focused on 2D relational reasoning, such as CLEVR [15] and GQA [12]. More recent efforts, like ScanQA [2], VSI-Bench [33], and MMSI-Bench [34], have systematically measured spatial reasoning in static 3D environments, often highlighting multi-image dependencies.

- **Dynamic Spatial Reasoning:** Acknowledging the limitations of static scenes, newer benchmarks have begun to address dynamics [30, 37]. VLM4D [39], for example, treats video as a four-dimensional modality to probe spatiotemporal correlations. However, this shift to dynamic scenes has exposed a critical flaw: multimodal hallucination. [16, 19, 28] have demonstrated that VLMs are highly prone to orientation hallucinations and semantic priors, especially when processing dynamic scenarios or uncommon viewpoints.

2.3. Future-Oriented World Models

A core application of WMs is the generation of physically plausible future videos for autonomous driving. Early explorations largely relied on fine-tuning pre-trained diffusion models [21, 29]. However, this path quickly revealed its limitations: many models either lacked essential planning and control components [26, 31, 38] or were constrained to low-resolution synthesis and short trajectories [10, 17], making them unsuitable for long-range forecasting.

To overcome these hurdles, recent research has pivoted to GPT-style autoregressive frameworks [6, 9, 32]. This new architecture has led to stronger temporal consistency and permits extended, multi-frame rollouts under continuous control.

Among the latest advancements, Epona [36] and DrivingWorld [11] represent two representative directions: Epona focuses on large-scale video-to-action pretraining for long-horizon driving imagination, while DrivingWorld incorporates explicit spatial constraints and controllable rollout strategies to stabilize world model predictions. Despite these advancements, the emphasis of current approaches remains centered on prediction. Although the synthesized videos often appear visually realistic, they frequently lack semantic fidelity, raising concerns about whether the predicted futures align with actual causal dynamics and scene semantics [4].

In this work, we introduce FSU-Bench, a unified benchmark designed to address the above limitations and enable a thorough assessment of the foresight capabilities of both VLMs and WMs.

3. FSU-QA

3.1. Foresight Intelligence

We use the term Foresight Intelligence to encapsulate the advanced predictive capabilities that go beyond simple pattern recognition or short-term forecasting. While “prediction” is often used in machine learning for tasks like next-token generation or immediate trajectory forecasting, “foresight” implies a deeper, more causal understanding. It is the ability to model, simulate, and evaluate complex, long-horizon futures, often involving multiple interacting agents

and counterfactual “what-if” scenarios. In essence, Foresight Intelligence goes beyond prediction — it enables models to envision and reason about complex, long-horizon futures through causal and counterfactual simulation.

Motivated by insights from cognitive neuroscience [22] and the demands of autonomous decision-making [24], we posit that Foresight Intelligence is supported by three foundational pillars:

- **Situational Modeling.** The ability to build a structured, semantic understanding of the current world state, including agent relationships and environmental constraints.
 - **Causal and Dynamic Simulation.** The core predictive engine that generates physically plausible and temporally coherent futures, including the ability to run “what-if” counterfactual scenarios based on causality.
 - **Goal-Oriented Planning and Evaluation.** The capacity to reason over these simulated futures to evaluate risks and opportunities, enabling the selection of an optimal action plan that ensures safety and achieves a specific objective.
- These three pillars collectively guide the design of FSU-Bench and are intrinsically woven into every task.

3.2. Overview

We introduce FSU-QA (see Fig. 1), a VQA dataset designed to train and quantitatively evaluate Foresight Intelligence in autonomous driving scenarios, where vehicles must operate in highly dynamic environments and anticipate future situations to ensure safety. FSU-QA aims to address two fundamental questions: (1) Whether current VLMs, which are primarily designed for perception and understanding tasks, possess the capability for Foresight Intelligence; and (2) Whether the visually realistic data generated by WMs can effectively contribute to developing Foresight Intelligence.

To address these two questions, we design two specialized evaluation paradigms on FSU-Bench. Both are cast as a question-answering task in which the model must answer future-related queries based on historical visual observations and motion trajectories.

VLM-oriented evaluation This evaluation is designed to assess the foresight understanding capability of a pre-trained VLM (\mathcal{VLM}):

$$\hat{a} = \mathcal{VLM}(q, V_{-T_h:0}, Traj_{-T_h:0}) \quad (1)$$

where \hat{a} is the predicted answer, q denotes the textual query, $V_{-T_h:0}$ refers to the historical video observations from $t = -T_h$ to the current time step ($t = 0$), and $Traj_{-T_h:0}$ represents the associated motion trajectories.

WM-oriented evaluation. This evaluation assesses the ability of WMs to produce semantically coherent data that can effectively support Foresight Intelligence. We quantify this contribution by measuring the performance improvements observed when integrating WM-generated outputs into the previously described VLM-oriented evaluation

framework:

$$\hat{a} = \mathcal{VLM}(q, V_{-T_h:0}, Traj_{-T_h:0}, \hat{V}_{1:T_f}, \hat{Traj}_{1:T_f}) \quad (2)$$

$$\hat{V}_{1:T_f}, \hat{Traj}_{1:T_f} = \mathcal{WM}(V_{-T_h:0}, Traj_{-T_h:0}) \quad (3)$$

where $\hat{V}_{1:T_f}$ and $\hat{Traj}_{1:T_f}$ are predicted future video and trajectory from WM (\mathcal{WM}).

4. Evaluation on FSU-Bench

4.1. Dataset Curation & Annotations

Building upon the nuScenes dataset [5], which provides rich sensory and map information, we develop an automatic data annotation pipeline to generate a high-quality dataset enabling both training and systematic evaluation of Foresight Intelligence, as illustrated in Fig. 3.

Scene Pre-processing and Representation. To approximate the driver’s perspective, we use videos recorded from the front-facing camera, each approximately 15 seconds long. We segment each video into a 3-second historical observation window and a 12-second future window. Because not every scene is valid for all tasks, we apply filtering to ensure annotation quality, yielding 18 to 28 questions per scene. The HD map is represented using lane lines.

Cognition-Inspired Task Design. To comprehensively train and evaluate Foresight Intelligence, we design nine tasks within FSU-QA (see Fig. 2), grouped into three major categories that span from low-level perception to high-level reasoning:

Spatio-temporal Dynamic Reasoning (low-level). This subset assesses the model’s capacity to capture dynamic spatio-temporal relations over long time horizons. It involves predicting the ego vehicle’s future motion states (both longitudinal and lateral) and understanding its interactions with nearby moving agents, characterized by variations in relative distance and position. This level comprises five tasks: Speed Change, Turn Change, Lane Change, Relative Distance (Rel. Dist.), and Relative Position (Rel. Pos.).

VRU-centric Risk Assessment (mid-level). This level assesses the model’s capability to detect and interpret Vulnerable Road Users (VRUs) and identify potential risk zones. It consists of three core annotation tasks:

- Pedestrian Intent (Ped. Int.). Annotate the intent of the closest front-view pedestrian within the next 0–3 seconds, based on trajectory and map information.
- Ego–VRU Relative Position Change (E–V Rel. Pos.). Label the final relative position of the closest VRU with respect to the ego vehicle at the end of the 0–3 second horizon.
- Risk Area. Classify the environmental risk level in the upcoming 3-second interval.

High-level Causal Reasoning (high-level). To mitigate nuScenes’ inherent “safety bias”, the limited presence of unsafe or hazardous driving cases, we introduce a Counterfactual Prediction (CFP) setting that evaluates a model’s sensitivity to unsafe behaviors and its capacity for causal understanding. For instance, consider the query: “If the ego vehicle were to turn left with a constant radius in the next 3 seconds, what would be the most likely outcome?” Such prompts allow us to directly assess the model’s causal reasoning ability, whether it can anticipate the safety implications of a prescribed action, such as predicting if a collision would occur.

QA Data Generation. For all nine tasks, we design a comprehensive question checklist using multi-sensor data, 3D object annotations, HD-map representations, and trajectory information. This checklist is applied to each scene to determine the tasks for which annotations are feasible, after which questions are generated via predefined templates. To produce the answers, we establish task-specific label systems and rule-based criteria. We extract and analyze ground-truth information, including kinematic states, spatio-temporal relations, VRU behaviors, environmental risks, and counterfactual verification results, from the dataset and HD-map. Mapping this information to the defined criteria enables systematic derivation of accurate answers for every question.

Specifically, we partition the entire video sequence and trajectory data into N segments of 3 seconds each, denoted as $S_{1:N}$. The first segment S_1 is regarded as the historical observation, whereas the subsequent segments $S_{2:N}$ represent future intervals. For QA generation, we randomly select a timestep i and construct a QA pair conditioned on $S_{1:i}$. This procedure yields QA pairs spanning varying temporal horizons, enabling evaluation of long-term foresight intelligence.

Quality Control. To ensure reliability, we designed a human-in-the-loop verification framework: human experts randomly sample scenes, provide detailed feedback on errors, and we subsequently modify the annotation logic or label corner cases individually. This two-way iteration maximizes the accuracy of annotations.

Additional information about the dataset curation process is provided in the *Supplemental Materials*.

4.2. Statistics & Analysis

FSU-QA contains more than 21K question–answer pairs generated from 850 real-world driving videos in the nuScenes dataset [5]. This ensures that FSU-QA robustly covers a wide spectrum of real-world driving scenarios, including different times of day, adverse weather conditions, and diverse urban geographies (Boston and Singapore). Among them, 18K QA pairs (700 scenes) are allocated for training, and 3K+ QA pairs (150 scenes) are



Figure 2. **Visualization of FSU-Bench.** Yellow boxes represent historical frames, and green boxes represent future frames. The bounding boxes are illustrative only and do not appear in the actual dataset. Content in {} is filled into a sentence template. Note: the questions above are simplified slightly for clarity and brevity.

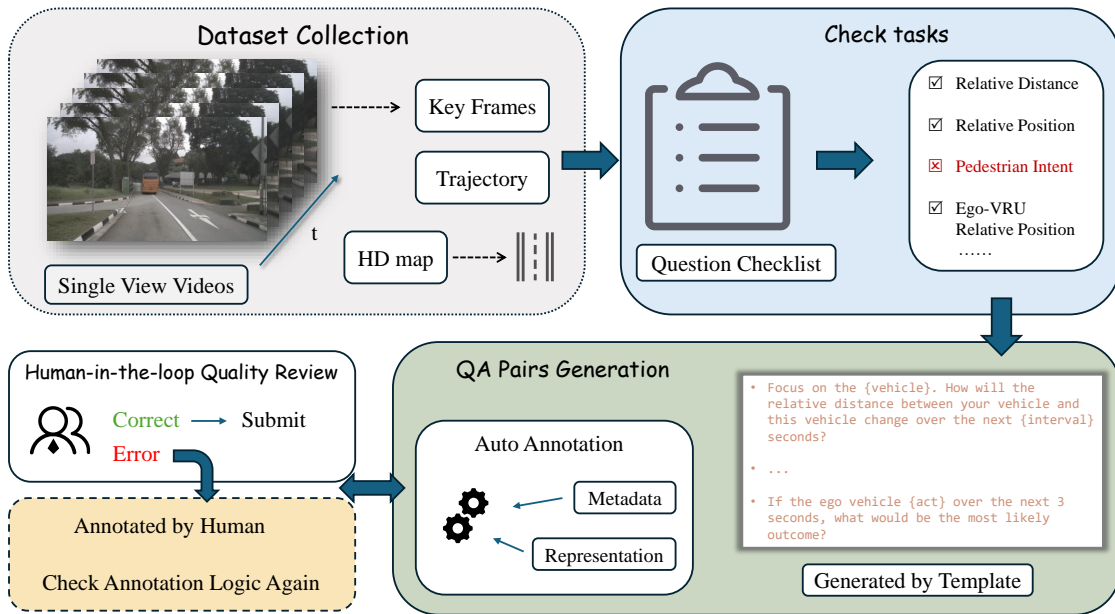


Figure 3. **FSU-QA construction pipeline.** Note: the questions above are simplified slightly for clarity and brevity.

held out for evaluation (FSU-Bench). An overview of the FSU-QA statistics is provided in Fig. 4.

4.3. Evaluation Setup

Benchmark Models. We conduct a comprehensive evaluation of a broad spectrum of Vision-Language Models (VLMs), spanning closed-source and open-source systems

Methods	Rank	Overall	Speed Change	Turn Change	Lane Change	Rel. Dist.	Rel. Pos.	Ped. Int.	E-V Rel. Pos.	Risk Area	CFP
			Low-level			Mid-level			High-level		
<i>Open-source Models</i>											
Qwen2.5-VL-72B	3	45.86	37.00	90.17	97.50	28.66	14.43	21.74	9.88	64.67	10.31
Qwen2.5-VL-7B	6	44.74	34.00	88.33	97.50	27.85	14.43	37.68	3.70	63.33	8.43
Qwen3-VL-32B	6	44.74	33.83	83.00	95.17	38.01	14.43	17.39	6.17	56.00	11.11
Qwen3-VL-8B	12	41.48	31.67	76.50	97.00	32.93	14.43	20.29	3.70	45.33	5.35
Llama 4 Maverick	4	45.47	41.83	66.00	92.00	33.74	18.50	36.23	18.52	42.67	24.36
Llama 4 Scout	11	41.95	41.67	70.33	81.50	30.69	14.43	36.23	3.70	50.67	16.06
<i>Closed-source Models</i>											
GPT-4o Mini	8	44.22	39.17	86.33	93.33	33.94	14.02	18.84	3.70	36.67	13.65
GPT-5	1	48.66	34.67	75.50	93.00	39.63	32.32	36.23	46.91	48.67	20.75
Gemini-2.0 Flash	13	41.43	32.00	74.17	91.17	33.54	15.04	30.43	7.41	29.33	12.45
Gemini-2.5 Flash	9	44.04	38.83	67.33	94.83	30.69	20.73	23.19	27.16	54.67	14.46
Gemini-2.5 Pro	9	44.04	37.83	66.17	91.67	35.37	22.76	30.34	37.04	25.33	18.47
Claude-3.7-Sonnet	5	45.00	31.83	84.67	92.67	35.16	16.67	33.33	19.75	44.00	14.59
Claude-Sonnet-4.5	2	46.38	37.17	76.67	94.50	35.77	20.33	27.54	14.81	49.33	19.54
<i>Finetuned Model</i>											
Qwen3-VL-8B-FI	-	59.59	43.67	92.33	93.17	38.21	39.63	28.99	38.27	66.00	50.20

Table 1. **Baseline Evaluation on FSU-Bench:** only input historical videos and trajectories. Dark gray cells indicate the best result across all models.

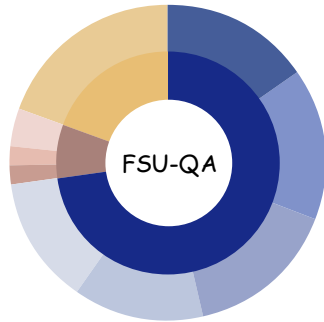
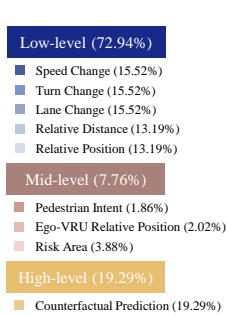


Figure 4. **FSU-QA Statistics.** The distribution of tasks across three levels.

of varying parameter sizes and architectural types, to reveal their capabilities in foresight intelligence.

For closed-source models, we assess *Gemini-2.0-Flash*, *Gemini-2.5-Flash*, *Gemini-2.5-Pro* [8], *GPT-4o-Mini* [13], *GPT-5*, *Claude-3.7-Sonnet-Standard*, *Claude-Sonnet-4.5*, *Llama-4-Scout*, and *Llama-4-Maverick* [1].

For open-source models, we evaluate *Qwen2.5-VL-72B-Instruct*, *Qwen2.5-VL-7B-Instruct* [3], *Qwen3-VL-32B-Instruct*, and *Qwen3-VL-8B-Instruct*.

To assess models’ capability to generate semantically coherent future data, we employ two representative world models: *Epona* [36], which integrates autoregressive and DiT components, and *DrivingWorld* [11], a purely autoregressive architecture. In the experiments, all previously mentioned VLMs serve as evaluators, enabling a comprehensive evaluation.

Metric Design. The questions are categorized into two

types: Multiple-Select Questions (MSQ) and Single-Select Questions (SSQ). We adopt *Accuracy (ACC)* as the evaluation metric. An answer is considered correct only when it exactly matches the ground truth; partial matches are not counted as correct.

5. Main Results

We follow the joint evaluation pipeline described in Sec. 3.2. Specifically, we first conduct the VLM-oriented evaluation to assess each VLM’s foresight intelligence and establish a baseline for subsequent comparisons. We then perform the WM-oriented evaluation, where the semantic coherence of WM-generated future data is quantified by the performance gains over this baseline.

5.1. VLM-oriented Evaluation

As shown in Eq. 1, the historical video sequence and trajectory are used as inputs to the VLM to generate future-related answers. For a thorough evaluation, we include two representative open-source models and three closed-source models with diverse configurations.

Closed-source Models. Closed-source models demonstrate overall stronger foresight reasoning capabilities compared to most open-source counterparts, with GPT-5 achieving the highest overall score (48.66) and securing Rank 1 among all evaluated models. Notably, GPT-5 shows clear advantages in mid-level spatio-temporal reasoning, indicating superior ability to understand dynamic interactions between agents. Claude-Sonnet-4.5 also performs competitively, ranking 2nd overall with strong results on Risk

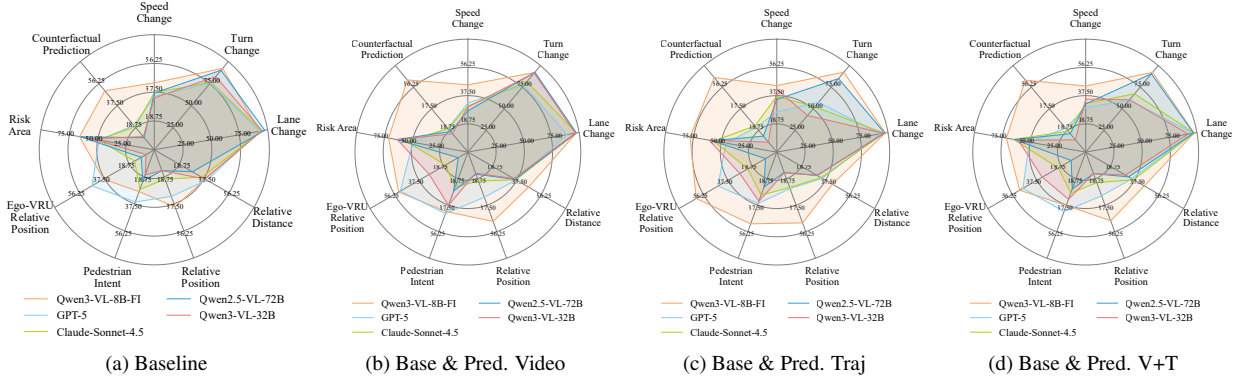


Figure 5. Results with data generated by *Epona*. (a)-(d) correspond to results under four different inputs.

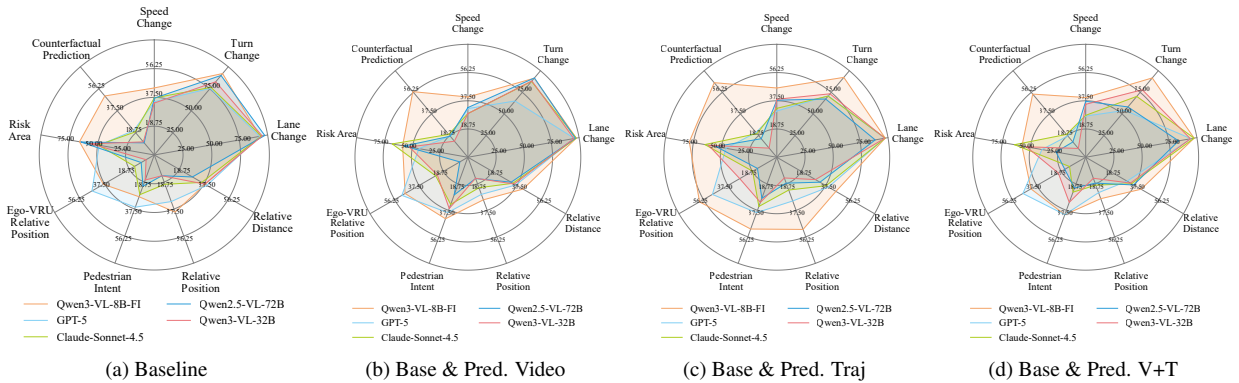


Figure 6. Results with data generated by *DrivingWorld*. (a)-(d) correspond to results under four different inputs.

Area (49.33) and Pedestrian Interaction (27.54), suggesting a heightened sensitivity to safety-critical cues. Meanwhile, Claude-3.7-Sonnet shows consistent mid-level performance but lags slightly behind Claude-Sonnet-4.5 in high-level reasoning. In contrast, Gemini models (2.0 Flash, 2.5 Flash, 2.5 Pro) exhibit more conservative performance, with overall scores around 41–44. Although they achieve reasonable results on tasks involving Lane Change and Turn Change, they struggle on more complex mid-level reasoning tasks such as E-V Relative Position and Risk Area, indicating limitations in modeling multi-agent dynamics. Finally, GPT-4o Mini, despite being a lightweight model, achieves competitive overall accuracy (44.22), surpassing some open-source models. This highlights that even small closed-source models retain strong temporal perception and high efficiency in low- and mid-level forecasting tasks. In summary, closed-source models collectively excel at mid- to high-level foresight reasoning, with GPT-5 and Claude-Sonnet-4.5 leading across most complex tasks. Their advantages are particularly pronounced in understanding dynamic agent relationships and safety-critical future events.

Open-source Models. Among open-source models, Qwen2.5-VL-72B achieves the best overall performance (45.86), ranking 3rd across all models. It exhibits strong ca-

pabilities on Low-level foresight tasks, particularly in Turn Change (90.17) and Lane Change (97.50), indicating that large Qwen models excel at recognizing imminent maneuver intentions from short-term visual cues. However, its performance drops noticeably on mid-level tasks, suggesting limited understanding of multi-agent spatial dynamics. Medium-sized models such as Qwen2.5-VL-7B and Qwen3-VL-32B deliver competitive overall scores (44.74), showing that open-source models can remain effective even at smaller scales. Nevertheless, they generally exhibit weaker high-level reasoning, revealing challenges in long-term, safety-critical forecasting. The Llama 4 series shows different behavior. Llama 4 Maverick performs well on mid-level tasks, but its high-level reasoning ability remains lower than closed-source models. Llama 4 Scout, despite being lightweight, maintains stable performance on foundational tasks, though its accuracy decreases on high-level prediction tasks. Overall, compared with closed-source models, open-source models excel in short-term and low-level maneuver prediction but struggle with complex multi-agent interactions and high-level future reasoning. This performance gap highlights the need for more effective long-range temporal modeling and better integration of semantic scene understanding in open-source VLMs.

Finetuning with FSU-QA. We further finetune Qwen3-VL-8B using FSU-QA, yielding the model Qwen3-VL-8B-FI. Although it is the smallest model in our evaluation, finetuning on FSU-QA significantly boosts its performance, allowing it to outperform all open-source and closed-source baselines. This result confirms that FSU-QA provides highly effective supervision for equipping VLMs with foresight intelligence.

5.2. WM-oriented Evaluation

We use the VLM-based evaluation as our baseline. Building on this, we further incorporate data generated by the world model and assess the semantic coherence of the synthesized samples through the resulting performance gains. In this evaluation, two representative world models are adopted. The results using data generated by *Epona* as input are shown in Fig. 5, while the results using data generated by *DrivingWorld* as input are shown in Fig. 6.

Future Augmentation with Epona. When predicted video is incorporated (b), all models show noticeable gains in tasks requiring short-term motion anticipation. In particular, GPT-5 benefits most from video cues, especially in Relative Distance and Ego-VRU Relative Position, indicating that video sequences effectively support mid-level dynamic understanding. With only predicted trajectories as additional input (c), the improvements shift toward relational reasoning. Models such as Claude-Sonnet-4.5 show larger gains in Pedestrian Intent and Risk Area, suggesting trajectory inputs provide clearer signals for future agent-agent interactions. Meanwhile, Qwen models exhibit more conservative improvements, implying a stronger reliance on visual cues. Finally, combining both predicted video and trajectories (d) yields the most comprehensive benefits. The finetuned Qwen3-VL-8B-FI achieves the most significant and uniform boosts across nearly all tasks, surpassing larger models in several categories such as Counterfactual Prediction and Ego-VRU Relative Position. This indicates that multi-modal predictive inputs effectively complement its finetuned foresight capability. GPT-5 also reaches its strongest performance in this setting, particularly in dynamic maneuver understanding (Turn Change, Lane Change). Overall, these results demonstrate that (1) predictive modalities enhance foresight reasoning in complementary ways—video for motion cues, trajectories for relational cues; and (2) models trained on FSU-QA, even with smaller parameter sizes, can substantially benefit from predictive inputs and outperform much larger closed-source systems.

Future Augmentation with Driving World. Similarly, using predicted video yields substantial improvements in categories related to motion dynamics and lane-level understanding. This implies that even short predicted video sequences help VLMs infer upcoming interactions and state

transitions. Meanwhile, predicted trajectories particularly benefit tasks involving Relative Position and Pedestrian Intent, where geometric consistency is crucial. These results highlight the complementary role of structured trajectory information in enhancing spatial reasoning precision. Third, combining both video and trajectory predictions achieves the most balanced gains across all dimensions. This fusion provides both rich visual context and accurate geometric cues, allowing the model to reason more comprehensively about future events, safety-critical scenarios, and “what-if” outcomes. The improvements in Risk Area and Ego-VRU Relative Position indicate that the additional future cues help VLMs better identify potential hazards and anticipate interactions that may unfold.

Across all settings, *DrivingWorld*-generated predictions consistently lead to larger performance gains for VLMs compared to *Epona*. Models benefit more from *DrivingWorld*’s future video and trajectory signals, especially on tasks requiring temporal consistency and agent-agent relational reasoning. In contrast, *Epona*’s predictions provide only modest improvements, indicating lower fidelity in motion and interaction modeling. Overall, *DrivingWorld* serves as a stronger and more informative world model, offering higher-quality predictive cues that substantially enhance downstream foresight reasoning across VLMs.

6. Future Work

In this work, we propose FSU-QA to facilitate research on Foresight Intelligence, a capability largely overlooked in prior studies. However, effective solutions for this problem remain underexplored. We highlight several promising research directions:

- Unified prediction-understanding VLMs. Developing VLMs that can jointly predict future videos and trajectories while performing high-level understanding tasks may offer a unified pathway toward foresight-capable models.
- Mutual enhancement between VLMs and WMs. Exploring how VLMs and WMs can benefit each other is another promising direction. For example, VLMs may help improve the semantic coherence of WM-generated data, while WMs can serve as supervisory signals to guide VLMs on Foresight Intelligence tasks.

7. Conclusion

In this work, we introduce FSU-QA, a VQA dataset for autonomous driving scenarios designed to advance research on Foresight Intelligence. A comprehensive evaluation on the accompanying FSU-Bench reveals that state-of-the-art VLMs still face significant challenges in anticipating future events. Furthermore, our benchmark uniquely assesses the semantic coherence of synthesized data by using VLMs to evaluate WM-generated predictions—an aspect largely neglected in previous work. In our experiments, fine-tuning

models on FSU-QA leads to substantial improvements in foresight understanding, demonstrating the dataset’s effectiveness and offering a principled foundation for future research.

References

- [1] Meta AI. Introducing llama 4: Advancing multimodal intelligence, 2025. 6
- [2] Daichi Azuma, Taiki Miyanishi, Shuhei Kurita, and Motoaki Kawanabe. Scanqa: 3d question answering for spatial scene understanding. In *2022 IEEE/CVF Conference on Computer Vision and Pattern Recognition (CVPR)*, pages 19107–19117, 2022. 2
- [3] Shuai Bai, Keqin Chen, Xuejing Liu, Jialin Wang, Wenbin Ge, Sibao Song, Kai Dang, Peng Wang, Shijie Wang, Jun Tang, Humen Zhong, Yuanzhi Zhu, Mingkun Yang, Zhao-hai Li, Jianqiang Wan, Pengfei Wang, Wei Ding, Zheren Fu, Yiheng Xu, Jiabo Ye, Xi Zhang, Tianbao Xie, Zesen Cheng, Hang Zhang, Zhibo Yang, Haiyang Xu, and Junyang Lin. Qwen2.5-vl technical report. *arXiv preprint arXiv:2502.13923*, 2025. 2, 6
- [4] Jake Bruce, Michael Dennis, Ashley Edwards, Jack Parker-Holder, Yuge (Jimmy) Shi, Edward Hughes, Matthew Lai, Aditi Mavalankar, Richie Steigerwald, Chris Apps, Yusuf Aytar, Sarah Bechtle, Feryal Behbahani, Stephanie Chan, Nicolas Heess, Lucy Gonzalez, Simon Osindero, Sherjil Ozair, Scott Reed, Jingwei Zhang, Konrad Zolna, Jeff Clune, Nando De Freitas, Satinder Singh, and Tim Rocktäschel. Genie: generative interactive environments. In *Proceedings of the 41st International Conference on Machine Learning*. JMLR.org, 2024. 3
- [5] Holger Caesar, Varun Bankiti, Alex H. Lang, Sourabh Vora, Venice Erin Liong, Qiang Xu, Anush Krishnan, Yu Pan, Giancarlo Baldan, and Oscar Beijbom. nuScenes: A Multimodal Dataset for Autonomous Driving. In *2020 IEEE/CVF Conference on Computer Vision and Pattern Recognition (CVPR)*, Seattle, WA, USA, 2020. IEEE. 4
- [6] Junyi Chen, Haoyi Zhu, Xianglong He, Yifan Wang, Jianjun Zhou, Wenzheng Chang, Yang Zhou, Zizun Li, Zhoujie Fu, Jiangmiao Pang, and Tong He. Deepverse: 4d autoregressive video generation as a world model, 2025. 3
- [7] An-Chieh Cheng, Hongxu Yin, Yang Fu, Qiushan Guo, Ruihan Yang, Jan Kautz, Xiaolong Wang, and Sifei Liu. Spatial-RGPT: Grounded spatial reasoning in vision-language models. In *The Thirty-eighth Annual Conference on Neural Information Processing Systems*, 2024. 2
- [8] Gheorghe Comanici, Eric Bieber, Mike Schaekermann, Ice Pasupat, Naveen Sachdeva, Inderjit Dhillon, Marcel Blstein, Ori Ram, Dan Zhang, Evan Rosen, et al. Gemini 2.5: Pushing the frontier with advanced reasoning, multimodality, long context, and next generation agentic capabilities. *arXiv preprint arXiv:2507.06261*, 2025. 6
- [9] Yaodong Cui, Shucheng Huang, Jiaming Zhong, Zhenan Liu, Yutong Wang, Chen Sun, Bai Li, Xiao Wang, and Amir Khajepour. Drivellm: Charting the path toward full autonomous driving with large language models. *IEEE Transactions on Intelligent Vehicles*, 9(1):1450–1464, 2024. 3
- [10] David Ha and Jürgen Schmidhuber. World models. 2018. 3
- [11] Xiaotao Hu, Wei Yin, Mingkai Jia, Junyuan Deng, Xiaoyang Guo, Qian Zhang, Xiaoxiao Long, and Ping Tan. Driving-World: Constructing World Model for Autonomous Driving via Video GPT. *arXiv preprint arXiv:2412.19505*, 2024. 3, 6
- [12] Drew A. Hudson and Christopher D. Manning. Gqa: A new dataset for real-world visual reasoning and compositional question answering. In *2019 IEEE/CVF Conference on Computer Vision and Pattern Recognition (CVPR)*, pages 6693–6702, 2019. 2
- [13] Aaron Hurst, Adam Lerer, Adam P Goucher, Adam Perelman, Aditya Ramesh, Aidan Clark, AJ Ostrow, Akila Welihinda, Alan Hayes, Alec Radford, et al. Gpt-4o system card, 2024. 6
- [14] Ayush Jain, Alexander Swerdlow, Yuzhou Wang, Sergio Arnaud, Ada Martin, Alexander Sax, Franziska Meier, and Katerina Fragkiadaki. Unifying 2d and 3d vision-language understanding. In *Forty-second International Conference on Machine Learning*, 2025. 2
- [15] Justin Johnson, Bharath Hariharan, Laurens van der Maaten, Li Fei-Fei, C. Lawrence Zitnick, and Ross Girshick. CLEVR: A Diagnostic Dataset for Compositional Language and Elementary Visual Reasoning. In *2017 IEEE Conference on Computer Vision and Pattern Recognition (CVPR)*, pages 1988–1997, Los Alamitos, CA, USA, 2017. IEEE Computer Society. 2
- [16] Yifan Li, Yifan Du, Kun Zhou, Jinpeng Wang, Xin Zhao, and Ji-Rong Wen. Evaluating object hallucination in large vision-language models. In *Proceedings of the 2023 Conference on Empirical Methods in Natural Language Processing*, pages 292–305, Singapore, 2023. Association for Computational Linguistics. 3
- [17] Hongbin Lin, Zilu Guo, Yifan Zhang, Shuaicheng Niu, Yafeng Li, Ruimao Zhang, Shuguang Cui, and Zhen Li. Drivegen: Generalized and robust 3d detection in driving via controllable text-to-image diffusion generation. In *Proceedings of the IEEE/CVF Conference on Computer Vision and Pattern Recognition (CVPR)*, pages 27497–27507, 2025. 3
- [18] Haotian Liu, Chunyuan Li, Qingyang Wu, and Yong Jae Lee. Visual Instruction Tuning. In *Advances in Neural Information Processing Systems*, pages 34892–34916. Curran Associates, Inc., 2023. 2
- [19] Wufei Ma, Haoyu Chen, Guofeng Zhang, Yu-Cheng Chou, Jieneng Chen, Celso M de Melo, and Alan Yuille. 3dsrbench: A comprehensive 3d spatial reasoning benchmark, 2025. 3
- [20] Muhammad Maaz, Hanoona Rasheed, Salman Khan, and Fahad Khan. Video-ChatGPT: Towards detailed video understanding via large vision and language models. In *Proceedings of the 62nd Annual Meeting of the Association for Computational Linguistics (Volume 1: Long Papers)*, pages 12585–12602, Bangkok, Thailand, 2024. Association for Computational Linguistics. 2
- [21] Robin Rombach, Andreas Blattmann, Dominik Lorenz, Patrick Esser, and Björn Ommer. High-resolution image synthesis with latent diffusion models. In *2022 IEEE/CVF Conference on Computer Vision and Pattern Recognition (CVPR)*, pages 10674–10685, 2022. 3

- [22] Daniel L. Schacter, Donna Rose Addis, and Randy L. Buckner. Remembering the past to imagine the future: the prospective brain. *Nature Reviews Neuroscience*, 8(9):657–661, 2007. 3
- [23] Yan Shu, Zheng Liu, Peitian Zhang, Minghao Qin, Junjie Zhou, Zhengyang Liang, Tiejun Huang, and Bo Zhao. Video-xl: Extra-long vision language model for hour-scale video understanding. In *2025 IEEE/CVF Conference on Computer Vision and Pattern Recognition (CVPR)*, pages 26160–26169, 2025. 2
- [24] R.S. Sutton and A.G. Barto. Reinforcement learning: An introduction. *IEEE Transactions on Neural Networks*, 9(5): 1054–1054, 1998. 3
- [25] Weiyun Wang, Zhangwei Gao, Lixin Gu, Hengjun Pu, Long Cui, Xingguang Wei, Zhaoyang Liu, Linglin Jing, Shenglong Ye, Jie Shao, Zhaokai Wang, Zhe Chen, Hongjie Zhang, Ganlin Yang, Haomin Wang, Qi Wei, Jinhui Yin, Wenhao Li, Erfei Cui, Guanzhou Chen, Zichen Ding, Changyao Tian, Zhenyu Wu, Jingjing Xie, Zehao Li, Bowen Yang, Yuchen Duan, Xuehui Wang, Zhi Hou, Haoran Hao, Tianyi Zhang, Songze Li, Xiangyu Zhao, Haodong Duan, Nianchen Deng, Bin Fu, Yinan He, Yi Wang, Conghui He, Botian Shi, Junjun He, Yingtong Xiong, Han Lv, Lijun Wu, Wenqi Shao, Kaipeng Zhang, Huipeng Deng, Biqing Qi, Jiaye Ge, Qipeng Guo, Wenwei Zhang, Songyang Zhang, Maosong Cao, Junyao Lin, Kexian Tang, Jianfei Gao, Haiyan Huang, Yuzhe Gu, Chengqi Lyu, Huanze Tang, Rui Wang, Haijun Lv, Wanli Ouyang, Limin Wang, Min Dou, Xizhou Zhu, Tong Lu, Dahua Lin, Jifeng Dai, Weijie Su, Bowen Zhou, Kai Chen, Yu Qiao, Wenhao Wang, and Gen Luo. InternV3.5: Advancing open-source multimodal models in versatility, reasoning, and efficiency. *arXiv preprint arXiv:2508.18265*, 2025. 2
- [26] Xiaofeng Wang, Zheng Zhu, Guan Huang, Xinze Chen, Jiayang Zhu, and Jiwen Lu. Drivedreamer: Towards real-world-driven world models for autonomous driving. *arXiv preprint arXiv:2309.09777*, 2023. 3
- [27] Yi Wang, Kunchang Li, Yizhuo Li, Yinan He, Bingkun Huang, Zhiyu Zhao, Hongjie Zhang, Jilan Xu, Yi Liu, Zun Wang, Sen Xing, Guo Chen, Junting Pan, Jiashuo Yu, Yali Wang, Limin Wang, and Yu Qiao. Internvideo: General video foundation models via generative and discriminative learning, 2022. 2
- [28] Zehan Wang, Ziang Zhang, Tianyu Pang, Chao Du, Hengshuang Zhao, and Zhou Zhao. Orient anything: Learning robust object orientation estimation from rendering 3d models. In *Forty-second International Conference on Machine Learning*, 2025. 3
- [29] Yuqing Wen, Yucheng Zhao, Yingfei Liu, Fan Jia, Yanhui Wang, Chong Luo, Chi Zhang, Tiancai Wang, Xiaoyan Sun, and Xiangyu Zhang. Panacea: Panoramic and controllable video generation for autonomous driving. In *2024 IEEE/CVF Conference on Computer Vision and Pattern Recognition (CVPR)*, pages 6902–6912, 2024. 3
- [30] Junbin Xiao, Xindi Shang, Angela Yao, and Tat-Seng Chua. Next-qa: Next phase of question-answering to explaining temporal actions. In *2021 IEEE/CVF Conference on Computer Vision and Pattern Recognition (CVPR)*, pages 9772–9781, 2021. 3
- [31] Zhenhua Xu, Yujia Zhang, Enze Xie, Zhen Zhao, Yong Guo, Kwan-Yee K. Wong, Zhenguo Li, and Hengshuang Zhao. DriveGPT4: Interpretable End-to-End Autonomous Driving Via Large Language Model. *IEEE Robotics and Automation Letters*, 9(10):8186–8193, 2024. 2, 3
- [32] Wilson Yan, Yunzhi Zhang, Pieter Abbeel, and Aravind Srinivas. Videogpt: Video generation using vq-vae and transformers. *2104.10157*, 2021. 3
- [33] Jihan Yang, Shusheng Yang, Anjali W. Gupta, Rilyn Han, Li Fei-Fei, and Saining Xie. Thinking in Space: How Multimodal Large Language Models See, Remember, and Recall Spaces. In *2025 IEEE/CVF Conference on Computer Vision and Pattern Recognition (CVPR)*, pages 10632–10643, Nashville, TN, USA, 2025. IEEE. 2
- [34] Sihan Yang, Runsen Xu, Yiman Xie, Sizhe Yang, Mo Li, Jingli Lin, Chenming Zhu, Xiaochen Chen, Haodong Duan, Xiangyu Yue, Dahua Lin, Tai Wang, and Jiangmiao Pang. Mmsi-bench: A benchmark for multi-image spatial intelligence, 2025. 2
- [35] Hang Zhang, Xin Li, and Lidong Bing. Video-LLaMA: An instruction-tuned audio-visual language model for video understanding. In *Proceedings of the 2023 Conference on Empirical Methods in Natural Language Processing: System Demonstrations*, pages 543–553, Singapore, 2023. Association for Computational Linguistics. 2
- [36] Kaiwen Zhang, Zhenyu Tang, Xiaotao Hu, Xingang Pan, Xiaoyang Guo, Yuan Liu, Jingwei Huang, Li Yuan, Qian Zhang, Xiao-Xiao Long, Xun Cao, and Wei Yin. Epona: Autoregressive diffusion world model for autonomous driving. In *Proceedings of the IEEE/CVF International Conference on Computer Vision (ICCV)*, pages 27220–27230, 2025. 3, 6
- [37] Ziang Zhang, Zehan Wang, Guanghao Zhang, Weilong Dai, Yan Xia, Ziang Yan, Minjie Hong, and Zhou Zhao. DSI-Bench: A Benchmark for Dynamic Spatial Intelligence. *arXiv preprint arXiv:2510.18873*, 2025. 3
- [38] Guosheng Zhao, Xiaofeng Wang, Zheng Zhu, Xinze Chen, Guan Huang, Xiaoyi Bao, and Xingang Wang. Drivedreamer-2: Llm-enhanced world models for diverse driving video generation. In *Proceedings of the Thirty-Ninth AAI Conference on Artificial Intelligence and Thirty-Seventh Conference on Innovative Applications of Artificial Intelligence and Fifteenth Symposium on Educational Advances in Artificial Intelligence*. AAAI Press, 2025. 3
- [39] Shijie Zhou, Alexander Vilesov, Xuehai He, Ziyu Wan, Shuwang Zhang, Aditya Nagachandra, Di Chang, Dongdong Chen, Xin Eric Wang, and Achuta Kadambi. Vlm4d: Towards spatiotemporal awareness in vision language models, 2025. 3

A. Task Descriptions

A.1. Task Definition

In this section, we provide detailed descriptions of each task defined in the dataset.

A.1.1. Spatio-temporal Dynamic Reasoning (Low-level)

Speed Change. This task evaluates the model’s capability to perceive and anticipate the longitudinal motion dynamics of the ego vehicle. Given historical visual observations and trajectories, the model is required to predict the trend of the ego vehicle’s speed over a specified time window (*e.g.*, the next 0~3s, 3~6s, or other intervals defined in the query). This is formulated as a classification problem, requiring the model to distinguish between acceleration, deceleration, or maintaining a constant speed.

Turn Change. This task assesses the model’s ability to perceive and anticipate the lateral motion dynamics of the ego vehicle. While the Speed Change task focuses on longitudinal control, Turn Change requires the model to predict the steering behavior over a specified time window based on historical context. The prediction is classified into four distinct categories: turn left, turn right, keep straight, or U-turn.

Lane Change. This task evaluates the model’s ability to anticipate the ego vehicle’s lane-changing behavior relative to the road topology. Distinct from the “Turn Change” task which relies on kinematic heading, “Lane Change” requires understanding the vehicle’s position within the HD map. Given historical observations, the model must predict whether the ego vehicle will change lanes within a specified time window.

Relative Distance. This task evaluates the model’s ability to perceive spatial depth and dynamic interactions between agents. Specifically, it focuses on predicting the change in distance between the ego vehicle and the nearest moving vehicle (in the front view). Given the historical context, the model must determine how the relative distance evolves over a specified time window.

Relative Position. This task focuses on the spatial directional relationship between the ego vehicle and the surrounding traffic. While “Relative Distance” estimates the depth, this task requires the model to categorize the direction of the nearest moving vehicle relative to the ego vehicle’s heading at the end of a specified time window. The relative position is discretized into 8 directional regions: ahead, behind, right, left, right-front, left-front, left-rear and right-rear.

A.1.2. VRU-centric Risk Assessment (Mid-level)

Pedestrian Intent. This task focuses on understanding the behavior of Vulnerable Road Users (VRUs). The model is required to identify the nearest pedestrian in the historical front view and predict their primary intention over the

next 3 seconds. The intent is classified into five critical behavioral modes: waiting at curbside, jaywalking, crossing in crosswalk, walking parallel to road and other irrelevant.

Ego-VRU Relative Position. This task is a specialized variant of the “Relative Position” task, explicitly focusing on Vulnerable Road Users such as pedestrians, cyclists, and motorcyclists. Given the historical context, the model must identify the nearest VRU and predict its spatial directional relationship relative to the ego vehicle at the end of 3 seconds. This task is critical for assessing safety risks, as VRUs often exhibit more flexible and unpredictable motion patterns than vehicles.

Risk Area. This task evaluates the model’s environmental awareness and its ability to anticipate potential hazards based on scene semantics. Instead of predicting immediate collisions, this task requires the model to classify the environmental risk level of the areas the ego vehicle will enter within a specified time window. The risk is categorized into three specific high-risk scenarios: VRU risk area, high occlusion area and complex intersection.

A.1.3. High-level Causal Reasoning (High-level)

Counterfactual Prediction. This task evaluates the model’s causal reasoning capabilities and its sensitivity to safety-critical scenarios. Unlike standard prediction tasks that ask about the actual future, this task presents a hypothetical “what-if” query: “If the ego vehicle were to perform action *A* (*e.g.*, turn left, accelerate) within a specified time window, what would be the most likely outcome?” The model must assess whether this hypothetical maneuver would lead to a collision, a traffic violation, or a safe outcome.

A.2. QA templates

We present the prompt templates organized by their cognitive complexity. Figs. 7 to 11 detail the templates for Low-level Spatio-temporal tasks, Figs. 12 to 14 for Mid-level Risk Assessment, and Fig. 15 for High-level Causal Reasoning.

A.3. Evaluation Prompt

We employed different prompts to evaluate the performance of VLMs and WMs under varied input conditions (see Figs. 16 to 19).

B. Implementation Details

B.1. Data Filtering

To ensure that every question in FSU-QA is valid and answerable, we implement a strict Task-Specific Filtering mechanism. We do not apply a generic filter; instead, we evaluate each frame against specific entry conditions for each of the nine tasks. A question is generated for a specific

QA Template: Speed Change

Question: You are an expert driving assistant. What is the speed change trend of the ego vehicle in the next `{interval}` seconds? The answer must be one of:

- A. Constant Speed
- B. Acceleration
- C. Deceleration

Answer: A/B/C

Figure 7. QA Template: Speed Change.

QA Template: Turn Change

Question: You are an expert driving assistant. What is the turn change trend of the ego vehicle in the next `{interval}` seconds? The answer must be one of:

- A. Straight
- B. Left turn
- C. Right turn
- D. U-turn

Answer: A/B/C/D

Figure 8. QA Template: Turn Change

task only if the scene satisfies the necessary prerequisites for that task.

B.2. Experiment Details

Hyperparameter Settings for Inference. To ensure a fair and robust evaluation, we adopted specific inference strategies tailored to the nature of the models.

API-based Models: This category includes both proprietary closed-source models (*e.g.*, GPT-5, Claude-Sonnet-4.5, Gemini-2.5) and hosted open-source models accessed via APIs (*e.g.*, Llama-4-Scout). For these models, we strictly adhered to the default settings provided by their respective official APIs. This approach ensures that we evaluate the representative “out-of-the-box” capabilities of these models as they are typically used by end-users and developers.

Locally Deployed Models: This category consists of the locally deployed Qwen series, with a precision of BF16. For these models, we utilized a low-temperature sampling strategy to balance determinism with generation stability. Specifically, we set the temperature to 0.1. This setting minimizes randomness to ensure consistent answers for scientific evaluation while retaining a slight probabilistic margin to prevent repetition loops often observed in strict greedy decoding modes.

Hyperparameter Settings for Finetuning. For the finetuned model Qwen3-VL-8B-FI, we performed full parameter fine-tuning on the LLM backbone and the vision-language projector, while keeping the vision encoder frozen. To manage the memory footprint of the 8B model

with long context windows, we utilized DeepSpeed ZeRO-3 optimization. The detailed training configuration is listed in Tab. 2.

B.3. Frequency Alignment

To effectively bridge the gap between high-frequency sensor data and the token limitations of VLMs, we implement a unified frequency alignment strategy.

Historical Frames. The raw visual data from the nuScenes dataset is recorded at 12 Hz. Directly feeding this dense stream into VLMs is computationally prohibitive. Therefore, we downsample the 3-second historical window to 2 Hz. Crucially, to fully capture the temporal boundaries of the observation window, we include both the start and end timestamps. This results in a sequence of 7 frames serving as the visual input for VLMs. This sampling strategy ensures that the model receives complete boundary information.

Future frames. Consistent with the input, the future frames are also sampled at 2 Hz for evaluation. We note that the native generation frequency of future frames depends on the World Model being evaluated. To ensure a standardized evaluation on FSU-Bench, we synchronize their generated outputs by sampling them to the same 2 Hz frequency before feeding them into the VLM.

C. Additional Quantitative Results

The joint evaluation results of *Epona* and VLMs are presented in Tab. 3, Tab. 4 and Tab. 5. While the joint eval-

QA Template: Lane Change

Question: You are an expert driving assistant. Will the ego vehicle change lanes in the next `{interval}` seconds? The answer must be one of:

- A. Left Lane Change
- B. Right Lane Change
- C. No Lane Change

Answer: A/B/C

Figure 9. QA Template: Lane Change.

QA Template: Relative Distance

Question: You are an expert driving assistant. Focus on the nearest `{description}` vehicle in front. How will the relative distance between your vehicle and this vehicle change over the next `{interval}` seconds? The answer must be one of:

- A. Approaching
- B. Distancing
- C. Maintaining
- D. Approaching then distancing

Answer: A/B/C/D

Figure 10. QA Template: Relative Distance.

QA Template: Relative Position

Question: You are an expert driving assistant with localization capabilities. Focus on the nearest `{description}` vehicle in front. Predict its relative position to the ego-vehicle over the next `{interval}` seconds. The answer must be one of the following eight:

- A. Ahead
- B. Behind
- C. Right
- D. Left
- E. Right-front
- F. Left-front
- G. Left-rear
- H. Right-rear

Answer: A/B/C/D/E/F/G/H

Figure 11. QA Template: Relative Position.

uation results of *DrivingWorld* and VLMs are presented in Tab. 6, Tab. 7 and Tab. 8.

D. Broader

The development of Foresight Intelligence in VLMs and WMs holds significant implications for the advancement of embodied AI and autonomous systems. In this section, we discuss the potential positive impacts and ethical considerations associated with our work, FSU-QA and FSU-Bench.

Advancing Safety in Autonomous Systems. The primary motivation behind FSU-QA is to enhance the safety

of autonomous driving. Traditional perception systems often focus on “what is happening now,” whereas safe driving necessitates anticipating “what will happen next.” By fostering research into Foresight Intelligence, specifically capabilities like Risk Area Assessment and Counterfactual Prediction, our work encourages the development of models that can proactively identify hazards and reason about “what-if” scenarios. This shift from reactive perception to proactive anticipation is a critical step toward reducing accidents and achieving Level 4/5 autonomy.

Ensuring Trustworthiness in Generative World Models. With the rapid rise of generative AI, World Models

QA Template: Pedestrian Intent

Question: You are an expert driving assistant with a focus on pedestrian behavior. Observe the closest pedestrian in the front view. What is their primary intent over the next 3 seconds? The answer must be one of:

- A. Waiting at Curbside
- B. Jaywalking
- C. Crossing in Crosswalk
- D. Walking Parallel to Road
- E. Other Irrelevant

Answer: A/B/C/D/E

Figure 12. QA Template: Pedestrian Intent.

QA Template: Ego-VRU Relative Position

Question: You are an expert driving assistant with localization capabilities. Focus on the closest VRU in the front view. Predict its relative position to the ego-vehicle after 3 seconds. The answer must be one of the following eight:

- A. Ahead
- B. Behind
- C. Right
- D. Left
- E. Right-front
- F. Left-front
- G. Left-rear
- H. Right-rear

Answer: A/B/C/D/E/F/G/H

Figure 13. QA Template: Ego-VRU Relative Position.

Hyperparameter	Value	Description
Base Model	Qwen3-VL-8B-Instruct	Initial checkpoint initialized from HuggingFace
Tuned Modules	LLM + Projector	Vision encoder is frozen (<code>tune_mm_vision=False</code>)
Optimization Strategy	DeepSpeed ZeRO-3	Memory optimization for full fine-tuning
Precision	BF16	Bfloat16 mixed precision training
Learning Rate	$2e - 5$	Peak learning rate
LR Scheduler	Cosine	Cosine decay with warmup
Warmup Ratio	0.05	Ratio of steps used for learning rate warmup
Weight Decay	0.01	Regularization parameter
Num Epochs	2	Total number of training epochs
Batch Size	32 (Global)	1 per device \times 4 accum steps \times 8 GPUs
Max Sequence Length	6000	To accommodate long video context
Computational Resources	8 \times NVIDIA A40	48GB VRAM per GPU

Table 2. **Hyperparameters for Finetuning Qwen3-VL-8B on FSU-QA.** We perform full parameter fine-tuning on the LLM backbone and projector while keeping the vision tower frozen.

are increasingly used to simulate future driving scenarios. However, a major risk is that these models may generate visually realistic but physically implausible or unsafe futures. FSU-Bench introduces a mechanism to evaluate the semantic coherence of generated data. By rigorously test-

ing whether generated futures align with causal logic and safety rules, our benchmark helps prevent the deployment of unreliable simulators and promotes the development of trustworthy World Models for safety-critical applications.

Limitations and Fairness. We acknowledge that the

QA Template: Risk Area

Question: You are an expert driving assistant with advanced situational awareness. Based on the current scene, which type(s) of high-risk area, if any, will the ego vehicle primarily enter within the next 3 seconds? Return the letter(s) corresponding to the selected option(s), separated by commas (e.g., 'A, B'). The answer may be one or more of:

- A. VRU Risk
- B. High Occlusion Area
- C. Complex Intersection
- D. No Risk Area

Answer: A, B (multiple correct answers)

Figure 14. QA Template: Risk Area.

QA Template: Counterfactual Prediction

Question: You are an expert driving assistant with predictive capabilities. If the ego vehicle were to {act} over the next 3 seconds, what would be the most likely outcome? This is a multiple-choice question, and the answer can be one or more of:

- A. Collision
- B. Driving Out of Legal Area
- C. Violating Traffic Rules
- D. Safe

Answer: A, B, C (multiple correct answers)

Figure 15. QA Template: Counterfactual Prediction.

data in FSU-QA, inherited from nuScenes, is geographically limited to specific urban environments (Boston and Singapore). Driving behaviors, traffic rules, and road infrastructures vary significantly across different countries and cultures. Consequently, models trained or evaluated on this benchmark may exhibit geographic bias and may not generalize perfectly to rural areas or developing regions with different traffic dynamics. We urge researchers and practitioners to exercise caution and perform extensive testing before deploying such models in unseen domains.

E. More Qualitative Visualization.

Visualizations for the nine task types are illustrated in Figs. 20 to 27.

Prompt: Baseline

```
Trajectory 1: [x, y, yaw]
⋮
Trajectory 7: [x, y, yaw]
Frame 1: {IMAGE_TOKEN}
⋮
Frame 7: {IMAGE_TOKEN}
The input image is captured by the vehicle's front-facing camera within 3
seconds.
The pose of each trajectory point corresponds to each image frame in sequence.
The trajectory points are relative coordinates, with the trajectory point of
the last frame as the origin; the yaw angles are also relative values, with
the yaw angle of the last frame as the reference.
Based on the input, Please answer the following questions in order. You only
need to answer with the option number, without providing the specific content
of the option.
Number each answer according to the question:
...
Definitions:
VRU_Risk means there is a vulnerable road user in the field of view that
warrants attention.
High_Occlusion_Area means the field of view will be highly occluded by large
vehicles.
Complex_Intersection means the ego vehicle will pass through an intersection
that contains at least three moving vehicles.
```

Figure 16. Prompt: Baseline.

Prompt: Base & Pred. Video

```
Trajectory 1: [x, y, yaw]
:
Trajectory 7: [x, y, yaw]
Historical Frame 1: {IMAGE_TOKEN}
:
Historical Frame 7: {IMAGE_TOKEN}
Predicted Frame 1: {IMAGE_TOKEN}
:
Predicted Frame 6: {IMAGE_TOKEN}
```

You are given two types of images:

1. Historical frames: 7 images captured by the vehicle's front-facing camera over 3 seconds. Each image corresponds to a historical trajectory point, in chronological order.
2. Predicted future frames: 6 images generated by a world model, representing possible future views of the vehicle in the next 3 seconds after the last historical frame.

The current moment is defined as the last historical frame. All trajectory points are historical and correspond to each historical frame. Trajectory points are provided as relative coordinates and yaw angles (x , y , radians), all relative to the last historical frame. The predicted future frames are provided to assist you in answering the following questions about possible future situations. Based on the input, please answer the following questions in order. You MUST ONLY reply with the option number for each question. Number your answers according to the question order:

...

Definitions:

VRU_Risk: A vulnerable road user is present and requires attention.

High_Occlusion_Area: The view will be highly occluded by large vehicles.

Complex_Intersection: The ego vehicle will pass through an intersection with at least three moving vehicles.

Figure 17. Prompt: Base & Pred. Video.

Prompt: Base & Pred. Traj

```
Historical Trajectory 1: [x, y, yaw]
:
Historical Trajectory 7: [x, y, yaw]
Historical Frame 1: {IMAGE_TOKEN}
:
Historical Frame 7: {IMAGE_TOKEN}
Predicted Trajectory 1: [x, y, yaw]
:
Predicted Trajectory x: [x, y, yaw] (x depending on outputs of WMs)
You are given three types of input:
1. Historical frames: 7 images captured by the vehicle's front-facing camera
over 3 seconds. Each image corresponds to a historical trajectory point, in
chronological order.
2. Historical trajectory: 7 trajectory points (relative coordinates and yaw
angles) corresponding to the historical frames, all relative to the last
historical frame.
3. Predicted trajectory: x trajectory points (relative coordinates and yaw
angles) predicted for the next 3 seconds after the last historical frame.
The current moment is defined as the last historical frame. All trajectory
points are relative to the last historical frame.
The predicted trajectory is provided to assist you in answering the following
questions about possible future situations within the next 3 seconds.
Based on the input, you must answer the following questions in order. You
can't refuse to answer! You MUST ONLY reply with the option number for each
question. Number your answers according to the question order:
...
Definitions:
VRU_Risk: A vulnerable road user is present and requires attention.
High_Occlusion_Area: The view will be highly occluded by large vehicles.
Complex_Intersection: The ego vehicle will pass through an intersection with
at least three moving vehicles.
```

Figure 18. Prompt: Base & Pred. Traj.

Prompt: Base & Pred. V+T

```
Historical Trajectory 1: [x, y, yaw]
:
:
Historical Trajectory 7: [x, y, yaw]
Historical Frame 1: {IMAGE_TOKEN}
:
:
Historical Frame 7: {IMAGE_TOKEN}
Predicted Trajectory 1: [x, y, yaw]
:
:
Predicted Trajectory x: [x, y, yaw] (x depending on outputs of WMs)
Predicted Frame 1: {IMAGE_TOKEN}
:
:
Predicted Frame 6: {IMAGE_TOKEN}
You are given four types of input:
1. Historical frames: 7 images captured by the vehicle's front-facing camera
over 3 seconds. Each image corresponds to a historical trajectory point, in
chronological order.
2. Historical trajectory: 7 trajectory points (relative coordinates and yaw
angles) corresponding to the historical frames, all relative to the last
historical frame.
3. Predicted future frames: 6 images generated by a world model,
representing possible future views of the vehicle in the next 3 seconds after
the last historical frame.
4. Predicted trajectory: x trajectory points (relative coordinates and yaw
angles) predicted for the next 3 seconds after the last historical frame.
These points do not necessarily correspond to the predicted frames one by one.
The current moment is defined as the last historical frame. All historical
trajectory points are relative to the last historical frame.
The predicted future frames and predicted trajectory are provided to assist
you in answering the following questions about possible future situations
within the next 3 seconds.
Based on the input, you must answer the following questions in order. You can't
refuse to answer! You MUST ONLY reply with the option number for each
question. Number your answers according to the question order:
...
Definitions:
VRU_Risk: A vulnerable road user is present and requires attention.
High_Occlusion_Area: The view will be highly occluded by large vehicles.
Complex_Intersection: The ego vehicle will pass through an intersection with
at least three moving vehicles.
```

Figure 19. Prompt: Base & Pred. V+T.

Methods	Rank	Overall	Speed Change	Turn Change	Lane Change	Rel. Dist.	Rel. Pos.	Ped. Int.	E-V Rel. Pos.	Risk Area	CFP
			Low-level			Mid-level			High-level		
<i>Open-source Models</i>											
Qwen2.5-VL-72B	5	47.30	27.33	92.33	97.50	36.18	15.65	27.54	7.41	64.00	17.80
Qwen2.5-VL-7B	10	43.38	25.33	92.33	97.50	27.64	14.43	42.03	3.70	46.00	8.43
Qwen3-VL-32B	3	47.45	30.00	91.33	96.67	35.16	14.84	37.68	29.63	63.33	15.93
Qwen3-VL-8B	11	43.17	29.67	87.17	92.17	35.37	14.63	39.13	9.88	60.67	3.75
<i>Closed-source Models</i>											
GPT-4o Mini	9	43.75	32.00	88.33	97.50	33.94	14.43	18.84	4.94	7.33	13.79
GPT-5	2	47.87	32.67	77.33	89.17	36.99	31.91	43.48	51.85	49.33	20.62
Gemini-2.0 Flash	8	46.12	33.67	91.33	97.50	36.99	14.43	26.09	16.05	50.00	9.77
Gemini-2.5 Flash	7	46.57	40.00	70.67	96.67	32.11	21.95	27.54	28.40	52.00	20.62
Gemini-2.5 Pro	6	47.14	37.17	83.50	97.00	28.86	21.95	36.23	38.27	34.00	19.14
Claude-3.7-Sonnet	3	47.45	33.33	91.17	97.33	35.16	17.89	28.99	17.28	45.33	16.60
Claude-Sonnet-4.5	1	48.39	29.00	87.67	97.50	34.55	21.54	33.33	24.69	68.00	19.81
<i>Finetuned Model</i>											
Qwen3-VL-8B-FI	-	65.81	44.67	92.00	97.50	46.54	48.98	42.03	53.09	71.33	62.52

Table 3. **Baseline & Pred. Video (from Epona) Evaluation on FSU-Bench:** Input historical frames, trajectories and predicted frames generated from Epona. Dark gray cells indicate the best result across all models.

Methods	Rank	Overall	Speed Change	Turn Change	Lane Change	Rel. Dist.	Rel. Pos.	Ped. Int.	E-V Rel. Pos.	Risk Area	CFP
			Low-level			Mid-level			High-level		
<i>Open-source Models</i>											
Qwen2.5-VL-72B	1	45.34	35.00	85.00	96.67	30.89	14.43	24.64	8.64	58.00	13.79
Qwen2.5-VL-7B	8	42.10	29.33	83.00	97.00	27.64	14.43	34.78	3.70	40.00	8.43
Qwen3-VL-32B	9	39.31	41.67	42.33	95.83	31.10	14.63	35.78	28.40	60.67	8.57
Qwen3-VL-8B	7	43.02	33.50	82.83	94.00	32.72	14.43	34.78	7.41	58.00	4.95
<i>Closed-source Models</i>											
GPT-4o Mini	4	43.57	34.50	86.83	96.50	34.35	14.43	20.29	3.70	4.00	13.25
GPT-5	6	43.11	26.66	57.45	93.05	34.88	25.81	36.23	45.12	45.70	21.41
Gemini-2.0 Flash	11	36.41	41.17	25.67	96.33	33.33	15.45	23.19	14.81	38.00	12.18
Gemini-2.5 Flash	10	38.76	37.76	31.50	96.67	32.52	16.06	26.09	30.86	48.00	18.21
Gemini-2.5 Pro	5	43.33	36.33	65.00	96.33	29.27	19.11	37.68	38.51	30.00	17.80
Claude-3.7-Sonnet	3	43.62	32.17	72.50	97.17	34.35	15.45	30.43	17.28	35.33	17.00
Claude-Sonnet-4.5	2	44.40	37.00	52.33	97.17	33.94	25.00	34.78	22.22	64.67	20.48
<i>Finetuned Model</i>											
Qwen3-VL-8B-FI	-	66.38	44.17	92.33	97.17	42.68	50.00	50.72	61.73	78.00	64.66

Table 4. **Baseline & Pred. Traj (from Epona) Evaluation on FSU-Bench:** Input historical frames, trajectories and predicted trajectories generated from Epona. Dark gray cells indicate the best result across all models.

Methods	Rank	Overall	Speed Change	Turn Change	Lane Change	Rel. Dist.	Rel. Pos.	Ped. Int.	E-V Rel. Pos.	Risk Area	CFP
			Low-level			Mid-level			High-level		
<i>Open-source Models</i>											
Qwen2.5-VL-72B	1	46.83	32.00	90.50	96.67	32.93	15.24	26.09	11.11	64.00	15.93
Qwen2.5-VL-7B	6	43.23	26.33	92.17	97.17	27.64	14.43	36.23	3.70	42.67	8.43
Qwen3-VL-32B	9	40.98	35.17	60.50	91.83	30.49	15.24	33.33	33.33	60.67	10.58
Qwen3-VL-8B	5	43.77	33.50	85.17	92.67	33.54	14.43	36.23	9.88	60.00	6.69
<i>Closed-source Models</i>											
GPT-4o Mini	8	42.86	30.00	84.83	96.50	36.18	14.43	18.84	3.70	4.67	13.65
GPT-5	3	45.42	29.50	60.17	96.17	35.37	30.89	42.03	48.15	50.67	20.75
Gemini-2.0 Flash	11	39.31	42.67	44.00	96.67	32.52	16.87	26.09	11.11	39.33	10.31
Gemini-2.5 Flash	10	40.30	41.33	35.00	96.17	34.55	14.63	23.19	23.46	60.00	19.01
Gemini-2.5 Pro	7	43.20	33.50	64.17	96.00	35.98	18.70	30.43	38.27	28.67	17.27
Claude-3.7-Sonnet	2	45.71	31.50	84.50	97.00	35.77	18.23	30.43	16.05	42.67	14.59
Claude-Sonnet-4.5	4	45.03	32.33	67.33	92.17	36.79	24.54	28.99	20.99	56.67	18.07
<i>Finetuned Model</i>											
Qwen3-VL-8B-FI	-	65.23	43.83	92.17	97.17	44.83	48.58	37.68	50.62	71.33	62.38

Table 5. **Baseline & Pred. V+T (from Epona) Evaluation on FSU-Bench:** Input historical frames, trajectories, predicted frames and trajectories generated from Epona. **Dark gray** cells indicate the best result across all models.

Methods	Rank	Overall	Speed Change	Turn Change	Lane Change	Rel. Dist.	Rel. Pos.	Ped. Int.	E-V Rel. Pos.	Risk Area	CFP
			Low-level			Mid-level			High-level		
<i>Open-source Models</i>											
Qwen2.5-VL-72B	1	47.17	33.00	91.67	96.33	33.13	15.04	24.64	6.17	57.33	18.21
Qwen2.5-VL-7B	10	43.12	25.17	92.17	97.17	27.64	14.43	37.68	3.70	44.00	8.43
Qwen3-VL-32B	3	45.63	29.00	88.17	95.00	35.57	14.84	36.23	23.46	52.67	13.92
Qwen3-VL-8B	11	41.06	30.17	80.33	88.50	31.50	14.63	36.23	11.11	57.33	4.28
<i>Closed-source Models</i>											
GPT-4o Mini	9	43.30	32.50	90.17	97.17	28.66	14.43	18.84	3.70	7.33	13.52
GPT-5	5	45.39	32.33	65.00	95.50	36.79	26.22	39.13	50.62	44.00	18.47
Gemini-2.0 Flash	7	44.22	29.50	87.17	94.67	38.21	16.46	18.84	4.94	44.67	9.77
Gemini-2.5 Flash	8	43.64	35.00	63.83	95.83	30.69	18.29	36.23	23.46	49.33	19.41
Gemini-2.5 Pro	6	44.69	34.67	71.50	95.67	32.52	20.73	31.88	30.86	26.67	20.35
Claude-3.7-Sonnet	4	45.58	30.00	90.00	97.17	32.93	15.45	24.64	18.52	33.33	16.47
Claude-Sonnet-4.5	2	47.01	30.50	81.33	97.17	36.59	20.53	24.64	17.28	55.33	20.35
<i>Finetuned Model</i>											
Qwen3-VL-8B-FI	-	60.35	40.00	91.83	97.17	42.28	30.08	43.48	48.15	58.67	56.89

Table 6. **Baseline & Pred. Video (from DrivingWorld) Evaluation on FSU-Bench:** Input historical frames, trajectories and predicted frames generated from DrivingWorld. **Dark gray** cells indicate the best result across all models.

Methods	Rank	Overall	Speed Change	Turn Change	Lane Change	Rel. Dist.	Rel. Pos.	Ped. Int.	E-V Rel. Pos.	Risk Area	CFP
			Low-level				Mid-level			High-level	
<i>Open-source Models</i>											
Qwen2.5-VL-72B	8	43.04	37.83	67.33	88.50	33.13	18.29	28.99	14.81	54.67	16.06
Qwen2.5-VL-7B	7	43.25	26.67	90.33	97.17	27.64	14.43	37.68	3.70	48.67	8.43
Qwen3-VL-32B	6	43.49	38.50	73.33	96.83	29.67	14.63	31.88	28.40	61.33	7.90
Qwen3-VL-8B	9	42.00	29.83	77.83	91.33	33.33	14.63	36.23	8.64	56.67	8.30
<i>Closed-source Models</i>											
GPT-4o Mini	5	43.77	34.50	88.83	97.00	31.50	14.43	18.84	4.94	5.33	13.92
GPT-5	1	48.11	30.67	71.00	96.67	39.63	30.89	39.13	49.38	52.67	21.42
Gemini-2.0 Flash	11	38.32	32.17	48.00	95.33	34.15	16.26	26.09	16.05	37.33	10.71
Gemini-2.5 Flash	10	40.80	32.00	46.33	97.17	32.32	20.73	31.88	30.86	50.67	16.87
Gemini-2.5 Pro	4	44.34	30.57	69.26	93.92	33.68	23.14	38.81	29.11	39.19	19.67
Claude-3.7-Sonnet	3	46.10	28.83	86.83	97.17	33.74	16.87	34.78	22.22	38.67	18.74
Claude-Sonnet-4.5	2	46.96	32.50	70.67	96.17	37.80	23.17	30.43	18.52	64.67	22.76
<i>Finetuned Model</i>											
Qwen3-VL-8B-FI	-	67.11	46.00	92.33	97.17	45.33	51.02	50.72	59.26	78.67	64.66

Table 7. **Baseline & Pred. Traj (from DrivingWorld) Evaluation on FSU-Bench:** Input historical frames, trajectories and predicted trajectories generated from DrivingWorld. **Dark gray** cells indicate the best result across all models.

Methods	Rank	Overall	Speed Change	Turn Change	Lane Change	Rel. Dist.	Rel. Pos.	Ped. Int.	E-V Rel. Pos.	Risk Area	CFP
			Low-level				Mid-level			High-level	
<i>Open-source Models</i>											
Qwen2.5-VL-72B	11	39.39	37.17	58.17	83.17	36.79	18.29	21.74	16.05	26.67	13.25
Qwen2.5-VL-7B	6	42.78	26.33	90.67	96.50	27.64	14.43	37.68	3.70	39.33	8.43
Qwen3-VL-32B	5	43.33	35.17	78.00	93.83	34.35	14.84	31.88	20.99	53.33	7.63
Qwen3-VL-8B	8	41.40	29.33	81.17	90.17	32.32	14.63	33.33	11.11	56.67	4.55
<i>Closed-source Models</i>											
GPT-4o Mini	3	43.98	34.17	92.00	97.00	30.49	14.43	20.29	4.94	6.67	12.99
GPT-5	7	41.71	27.33	54.17	94.33	31.71	25.00	40.58	48.15	39.33	18.47
Gemini-2.0 Flash	10	39.62	32.17	59.67	32.00	36.38	17.48	27.54	13.58	36.67	8.70
Gemini-2.5 Flash	9	40.82	28.83	48.33	95.67	32.52	18.29	27.54	22.22	54.67	21.15
Gemini-2.5 Pro	4	43.51	32.33	69.50	95.17	30.49	18.09	30.43	28.40	33.33	20.35
Claude-3.7-Sonnet	1	45.58	29.00	85.83	97.17	33.74	16.46	28.99	20.99	37.33	17.94
Claude-Sonnet-4.5	2	44.71	27.83	70.33	97.17	35.16	19.72	24.64	12.35	64.00	19.81
<i>Finetuned Model</i>											
Qwen3-VL-8B-FI	-	59.54	39.67	91.67	97.17	42.48	29.27	40.58	41.98	57.33	54.75

Table 8. **Baseline & Pred. V+T (from DrivingWorld) Evaluation on FSU-Bench:** Input historical frames, trajectories, predicted frames and trajectories generated from DrivingWorld. **Dark gray** cells indicate the best result across all models.



Figure 20. **Speed Change Visualization. Top: Constant Speed. Bottom: Acceleration.**



Figure 21. **Turn Change Visualization. Top: Turn Right. Bottom: Turn Left.**



Figure 22. **Lane Change Visualization. Top: Left Lane Change. Bottom: Right Lane Change.**

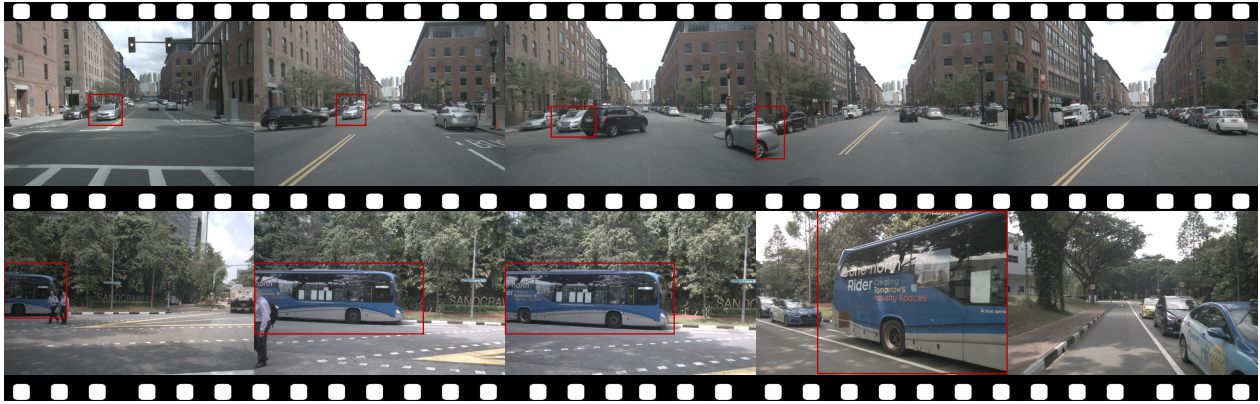


Figure 23. **Relative Distance & Relative Position Visualization.** The bounding boxes are illustrative only and do not appear in the actual dataset.



Figure 24. **Pedestrian Intent Visualization.** **Top:** Waiting at curbside. **Bottom:** Jaywalking. The bounding boxes are illustrative only and do not appear in the actual dataset.



Figure 25. **Ego-VRU Relative Position Visualization.** **Top:** Motorcyclist. **Bottom:** Pedestrian. The bounding boxes are illustrative only and do not appear in the actual dataset.



Figure 26. **Risk Area Visualization.** **Top:** High Occlusion Area. **Bottom:** Complex Intersection.



Figure 27. **Counterfactual Prediction Visualization.** **Top:** What would happen if the ego vehicle were to change lanes to the left? **Bottom:** What would happen if the ego vehicle were to turn right?